Chapter 4

Grinding Force of Cylindrical and Creep-Feed Grinding Modeling

Pavel Kovač and Marin Gostimirović

Additional information is available at the end of the chapter

http://dx.doi.org/10.5772/intechopen.76968

Abstract

This chapter presents an experimental study of grinding forces as relationship of workpiece speed v, feed rate s_a and depth of cut a. For the modeling of cylindrical grinding used was response surface methodology and genetic algorithms. Modeled was the tangential force F_t and the normal force F_n in cylindrical grinding. The process included measurement of cutting forces during cylindrical grinding and later calculating their values using abovementioned techniques and determined adequate models. This chapter also examines the value and character of cutting forces in the creep-feed grinding. In order to identify the impact of cutting forces on the state of the process of creep-feed grinding, according to the elements of the machining experimental tests, relationship of the tangential and normal components of the grinding force and ratio of grinding force were determined. In comparison with the traditional multi-pass grinding results, the occurrence of higher cutting forces in creep-feed grinding, especially normal components, is shown.

Keywords: cutting force, cylindrical grinding, modeling, genetic algorithms, creep-feed grinding

1. Introduction

Knowledge about machinability of materials parameters, tool wear, quality of machined surface, cutting temperature, cutting forces, and so on, is beneficial not only for cutting process but also for designing the machine tools, fixtures, tools and process management. This was the goal of many researches especially in cutting, but there are only few data regarding grinding [1].

Research in grinding is performed with the purpose to define machining parameters, roughness of machined surface, grinding forces and grinding temperatures [2, 3]. Forces in surface grinding are measured with dynamometer Kistler, and they are increasing with increase of the material removal rate. Cutting forces measurements, during cylindrical grinding, are realized with dynamometer Kistler and are shown in [4].

Mathematical models of grinding force and grinding temperature for three wheels were established in [3]. Then, the role of chip formation force and friction force in grinding was investigated, and the thermal distribution in contact zone between workpiece and wheel was analyzed based on the mathematical model.

Grinding process is generally used to improve the tolerance integrity and surface integrity of a workpiece. It is crucial to know process forces since they are necessary to identify the conditions for surface burn. In [5], a new semi-analytical force model for grinding process was developed by modeling abrasive grits and their interaction with the workpiece material. Semi-analytical equations for normal and tangential force components as well as average force per grit are established by using the micro milling analogy. The model can then be used in prediction of the forces for different cases involving the same material and the abrasive grain however with different conditions.

In [6], a new grinding force model was developed by incorporating the effects of variable coefficient of friction and ploughing force. This is based on the fact that chip formation during grinding consists of three stages: ploughing, cutting and rubbing. Equations for the total normal and tangential force components per unit width of the grinding during these three stages were established. These components were expressed in terms of the experimental coefficients and process parameters like wheel speed, table feed and depth of cut. All the coefficients were determined experimentally by performing grinding tests at specified conditions according to the experimental trifactorial central composition plan.

Investigation of grinding force and grinding temperature of ultra-high-strength steel Aermet 100 in conventional surface grinding using a single alumina wheel, a white alumina wheel and a cubic boron nitride wheel was done in [7]. First, mathematical models of grinding force and grinding temperature for three wheels were determined. Then, the role of chip formation force and friction force in grinding force was investigated and thermal distribution in contact zone between workpiece and grinding wheel was analyzed based on the mathematical model. The experimental result indicated that the ratio of minimum grinding force to the maximum grinding force under the same grinding parameters can be achieved when using a CBN wheel and a single alumina wheel, respectively.

Proper understanding of the grinding forces can be useful in designing grinding machine tools and fixtures. Additionally, information on specific energy helps in selecting process parameters for achieving optimum output [8]. In this chapter, analysis of the effects of process parameters, tribology, work material and auxiliary equipment on grinding forces and specific energy, has been carried out. Existing models have been critically analyzed, and Werner's specific force model was found to be quite promising for advanced grinding processes. It was found that under specific boundary conditions and environment similar to advanced grinding processes, this model estimates grinding forces with acceptable accuracy [9].

Optimal control of workpiece thermal state in creep-feed grinding using inverse heat conduction analysis was done in [10] and surface layer properties of the workpiece material in high-performance grinding were analyzed in [11]. An inverse heat transfer problem for optimization of the thermal process in machining was done in [12].

For determination of dependence between cutting forces and machining parameters, firstly the full factorial experiment second-order design is used by [13]. With this approach, it is possible to determine the dependence of machining parameters and the results with minimal number of experiments.

This chapter analyzes the cutting forces in the creep-feed grinding and experimentally determined mean values of cutting force of abrasive grains that are currently in the grip with the workpiece as well. Cutting forces are determined depending on the treatment regime for two types of corresponding wheels.

As a second option for modeling, the dependence functions are genetic algorithms. They are extensively described in [14], and the same principle is implemented in this chapter.

1.1. Genetic algorithms

Genetic algorithms (GA) mimic the process of natural evolution by incorporating the "survival of the fittest" philosophy. In GA, a point in search space (binary or decimal numbers) is known as chromosome. A set of chromosomes is called population. A population is operated by three fundamental operations as follows:

1. reproduction (to replace the population with large number of good strings having high-fitness values)
2. crossover (for producing new chromosomes by combining the various pairs of chromosomes in the population).
3. mutation (for slight random modification of chromosomes).

At the very beginning, an initial population of 50 individuals is created. They are randomly generated from interval 0–1 using uniform distribution for creation of population. This indicates that real number coding was used. As a fitness scaling function, rank method was used. Most fit individual with the best raw score is assigned as first on the scaling list. Next to fittest is ranked number 2 and so on. This method is ranking every individual in generation as compared to the best individual in that same generation, no matter how good or bad fitness value is. And It was selected because it allowed the fastest convergence toward the best solution.

Selection of individuals for presence in mating pool was executed by roulette wheel method. Size of area on wheel occupied by a single individual is defined by rank score—the better the score, the bigger the area. Wheel is then spun and individual with the largest area has the most chances to be assigned a slot in mating pool. This action is repeated until all slots in mating pool are assigned. In each generation, two of the best individuals are automatically transferred to next generation. This act is called elitism and it guarantees that best genetic material is passed onto next generation. By setting this parameter high, the genetic diversity

is quickly reduced which leads to prolonged convergence time. On the other hand, setting it low, elite genetic material of every generation may be lost and algorithm stuck in local minimum. Number of individuals created by heuristic crossover is, in this case, 43. Heuristic crossover is carried out by creating children that randomly lie on the line containing the two parents, a small distance away from the parent with the better fitness value and in the direction away from the parent with the worse fitness value. After transferring two elite individuals from previous generation and creating 43 by crossover to complete a full population with 50 members last 5 individuals are created by mutating 5 of their predecessors.

With the process of mutation, a completely new genetic material is introduced into the population which helps in expanding genetic diversity and search space. It also prevents jamming an algorithm in a local minimum of the function. Uniform mutation is selected with the rate of 0.2. This type of mutation is basically a two-step process. In the first step, the algorithm selects a gene of an individual for mutation where each gene has the same probability as the mutation rate of being mutated. In the second step, the algorithm replaces each selected entry by a random number selected uniformly from the range for that entry. This whole process of selection, recombination and mutation lasted 500 generations.

2. Experimental investigation

2.1. Mathematical model

The abovementioned methodology of trifactorial central composition plan design was used during investigation in cylindrical grinding. Input parameters during modeling were machining parameters:

- Workpiece speed v (m/min)
- Feed rate s_a (mm/rev)
- Depth of cut a (mm)

Output parameters were:

- Tangential force F_t (N)
- Normal force F_n (N)

Other parameters were kept constant: tool geometry, tool wear, cooling and lubricating fluid, dynamical system machine-tool-workpiece.

Chosen mathematical model for grinding forces has the form:

$$F_i = C.v_r^x.s_a^y.a^z. \quad (1)$$

2.1.1. Creep-feed grinding

In the case of surface grinding, where there is no lateral movement of the table, usually resulting force has been divided into tangential (extensive) component F_t and normal (radial) component F_n [6, 15].

Tangential component acts in the direction of the tangent to the surface of the grinding wheel and workpiece contact, that is, in the direction of cutting speeds. The normal component acts normally to the surface of the wheels and workpiece. As the diameter of the wheel is far greater than the depth of cut, it can be assumed that the tangential and normal component supine in a horizontal or vertical plane, **Figure 1**.

The relationship of normal and tangential components of the grinding forces is defined as the grinding force ratio:

$$\lambda = \frac{F_n}{F_t} = \frac{F_n'}{F_t'} \tag{2}$$

In the previous equation, the components of the grinding forces are reduced per unit width of grinding *b*, referred to as the specific grinding force:

$$\begin{aligned} F_t' &= \frac{F_t}{b} \\ F_n' &= \frac{F_n}{b} \end{aligned} \tag{3}$$

Grinding force can be expressed by specific grinding energy, which shows how much energy is consumed per unit volume of material removed:

$$u = \frac{P'}{Q'} = \frac{F_t' \cdot v_s}{a \cdot v_w} = \frac{F_t'}{h_m} \tag{4}$$

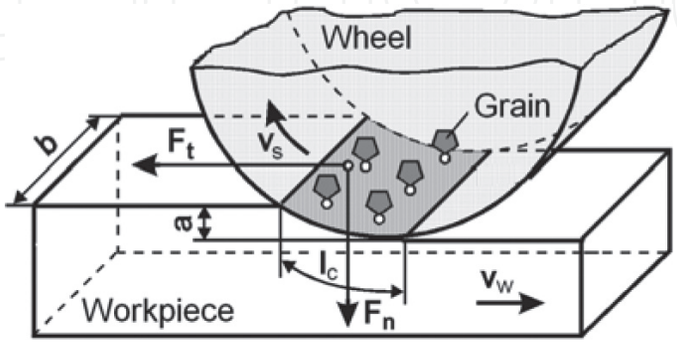

Figure 1. Components of the cutting force during creep-feed grinding.

2.2. Conditions during the experiment

2.2.1. Cylindrical grinding

Workpieces were cylindrical shaped Ø 60 × 150 mm and were made from two types of steel:

- Steel EN 34Cr4. with mechanical properties R_{p02} = 460 MPa; R_m = (690–840) MPa
- Steel EN 18CrNi8. with mechanical properties $R_{p0.2}$ = 485 MPa; R_m = (1080–1330) MPa

Tool was cylindrical grinding wheel Ø 350 × 40 × 127 mm, type B60L6V. Machining was performed on cylindrical grinder by manufacturer LŽTK Kikinda type UB, with dimensions of the workplace 1000 × 400 mm and power was rated 4 kW. Cutting speed was kept constant at v_s = 3.65 m/s. Varied machining regime parameter values: work speed v_r, feed rate s_a and depth of cut a are shown in **Table 1**.

2.2.2. Creep-feed grinding

Workpiece material used in the experimental setup was the molybdenum high-speed steel (HSS), which is widely used in the industry of cutting tools. Designation of the selected speed steel is DIN S 2-10-1-8. This steel belongs to a group of ledeburite steel with a microstructure consisting of martensite and fine mixtures of primary and secondary ledeburite cementite. The chemical composition of the test material was: 1.08% C; 0.22% Si; 0.23% Mn; 0.014% P; 0.019% S; 4.1% Cr; 1.5% W; 9% Mo; 1.1% V and 8% Co. Measured hardness on all samples ranged 66 ± 1 HRC. Experimental samples consisted of tiles measuring 40 × 20 × 16 mm.

Based on the recommendations, the chosen material of the workpiece and set the conditions of processing were selected two wheels similar characteristics: wheels "Norton" type 32A54 FV BEP and size 400 × 80 × 127 mm, respectively "Winterthur" type 53A80 F15 V PMF and size 400 × 50 × 127 mm. The wheels are with high-quality abrasive grain, medium grain size, hardness soft, open structure with ceramic binder. All experiments were conducted with sharp wheels, and sharpening is done with a diamond planer alignment with a depth of 0.01 mm/ speed and displacement of 0.1 mm/rev.

The machining conditions included variable depths of cut and workpiece speed. The depth of cut was a = 0.05; 0.1; 0.25; 0.5; 1 mm and the workpiece speed was v_w = 2.5; 5; 10; 25; 50 mm/s. The adopted mean value of specific material removal rate is Q' = 2.5 mm^3/mm·s. The grinding wheel speed was constant v_s = 30 m/s.

2.3. Measurement of grinding force components

2.3.1. Cylindrical grinding

Resulting grinding force can be divided into three components (**Figure 2**):

- Tangential component F_t (acts in vertical direction)
- Normal component F_n (acts horizontally)
- Axial force F_a (acts in the direction of workpiece axis-feed)

No.	Machining factor			Experimentally measured values				Calculated values by response surface methodology			
				EN 18CrNi8		EN 34Cr4		EN 18CrNi8		EN 34Cr4	
	v_r [m/min]	s_a [mm/rev]	a [mm]	F_t [N]	F_n [N]	F_t [N]	F_n [N]	F_t [N]	F_n [N]	F_t [N]	F_n [N]
1	18.4	20	0.01	11.8	17	10.9	17.8	12.31	20.36	11.87	20.48
2	36.8	20	0.01	12.4	17.8	11.8	19.8	12.67	21.43	12.39	21.71
3	18.4	30	0.01	12.3	18.4	13	18.9	12.56	21.40	12.42	20.97
4	36.8	30	0.01	12.9	19.8	13.2	21.1	12.92	22.53	12.97	22.23
5	18.4	20	0.02	16.1	29	17.4	29	15.37	28.23	15.64	27.51
6	36.8	20	0.02	16.6	31.5	17.9	31.2	15.81	29.71	16.33	29.16
7	18.4	30	0.02	17.2	31.2	18.8	33.1	15.68	29.66	16.36	28.16
8	36.8	30	0.02	17.5	33.3	20	33.6	16.13	31.22	17.09	29.86
9	26	25	0.014	12.1	25.4	12.3	24.8	14.06	25.16	14.22	24.65
10	26	25	0.014	12	25.3	13.5	24.7	14.06	25.16	14.22	24.65
11	26	25	0.014	12.6	24.5	12.2	24	14.06	25.16	14.22	24.65
12	26	25	0.014	12.8	24.3	14	24.1	14.06	25.16	14.22	24.65
13	16	25	0.014	13.6	23.1	12.6	22.8	13.79	24.27	13.79	23.66
14	42.4	25	0.014	14.2	25.6	13.6	25.6	14.35	26.08	14.66	25.69
15	26	18.4	0.014	14.4	22.1	12.4	23.1	13.85	24.23	13.74	24.21
16	26	32.6	0.014	15.5	28.2	14.1	24.3	14.25	25.99	14.64	25.03
17	26	25	0.0086	11	19.2	10.8	19	12.03	20.00	11.71	20.03
18	26	25	0.023	17.1	33.2	18.1	31.1	16.48	31.78	17.32	30.45
19	16	25	0.014	13.4	23	12.1	22.5	13.79	24.27	13.79	23.66
20	42.4	25	0.014	14.5	25.8	13.9	25.7	14.35	26.08	14.66	25.69
21	26	18.4	0.014	14.2	22.9	12.6	23.3	13.85	24.23	13.74	24.21
22	26	32.6	0.014	15	28.1	14.6	24.1	14.25	25.99	14.64	25.03
23	26	25	0.0086	11.1	19.2	11	19.6	12.03	20.00	11.71	20.03
24	26	25	0.023	17.6	33.3	18.5	31.8	16.48	31.78	17.32	30.45

Table 1. Measured and calculated values of cutting forces.

During cylindrical grinding, axial force component F_a can be neglected because it is minor in comparison with F_t, which allows a much simpler dynamometer design.

Until now, two-component dynamometer with strain gauges was used for cylindrical grinding force monitoring. The same will be used in this experiment. Strain gauges were placed on both centers which enable reliable and accurate measurement of both components of cutting force on whole length of the workpiece.

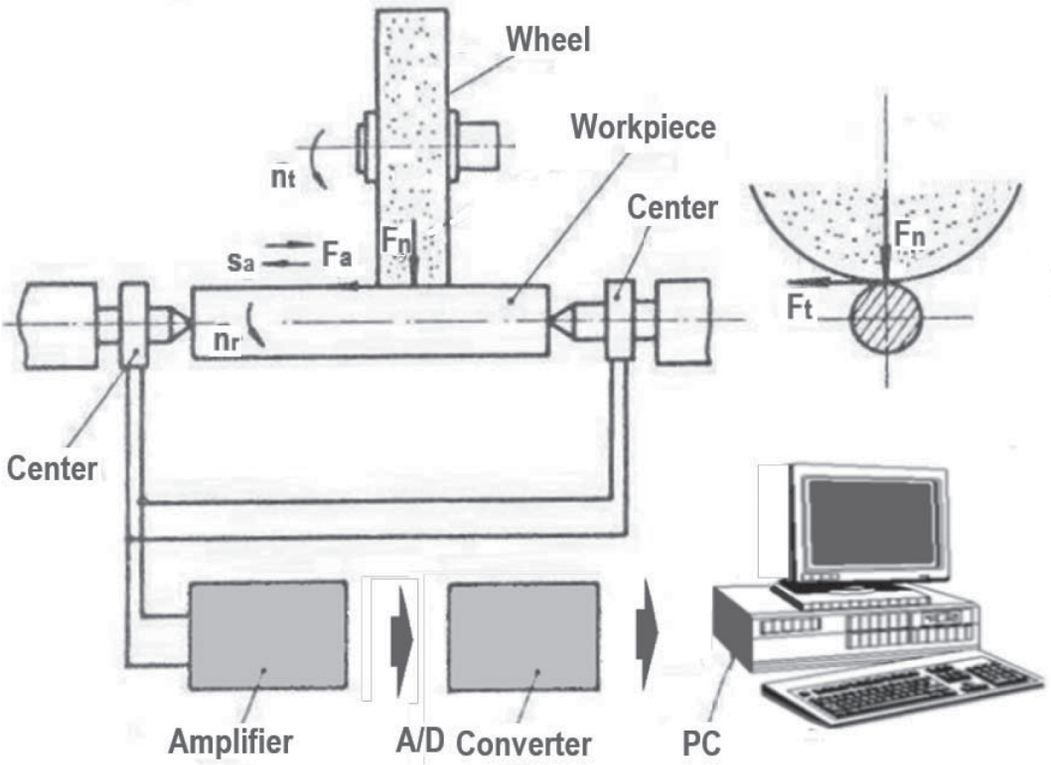

Figure 2. Information system for monitoring and processing cutting forces during cylindrical grinding.

Dynamometers were constructed in the manner that four strain gauges were taped onto cylindrical part of the center. In this way, two of the strain gauges are in the horizontal direction and two are in the vertical direction. All strain gauges are connected to bridge, so every component can be measured independently.

During grinding, under the influence of cutting forces, centers are deformed in the vertical and horizontal planes which are measured by strain gauges. Deformation of the strain gauge is proportional to load and signals coming from them have to be amplified and registered. To determine the cutting resistance values, dependence between measured signal (voltage on bridge) and load, $F_i = f(U)$, is determined with the use of lever and weight.

Mentioned measurement technique is accurate enough, but some things have to be considered:

- Quality of the glue used to stick strain gauges onto revolving centers
- Possible differences between electrical properties of strain gauges
- Accuracy of strain gauges positioning into vertical and horizontal planes
- Protecting the strain gauges from environmental influence
- Quality of the acquisition system
- Length of the cables to transfer measured signal

During the experiment, standard cemented carbide revolving centers are used.

Signals from dynamometers on centers were amplified with Kistler CA 5001 amplifier. Afterward, those signals were transformed by A/D converter to PC computer for further processing and analysis of measured data, **Figure 2**.

2.3.2. Creep-feed grinding

Measuring the forces that occur during creep-feed grinding was done using three-component dynamometers "Kistler Instrument AG," type 9257. The used dynamometer works on the piezoelectric principle, which is reflected in the emergence of electricity on the surface of the crystal plate embedded in the dynamometer when the same force exerted pressure. Electricity is amplified by means of amplifiers capacitive "Kistler," type CA 5001 and then is converted into DC voltage in the range from 0 to 10 V.

Measurement, analysis and control of the grinding force were performed using the information of the measuring system [10], where data acquisition is implemented by AD cards and cash integrated software package, **Figure 3**. The set information measurement data acquisition system is characterized by a high degree of accuracy, reliability, speed of response and the ability to reproduce measurement results. It allows real-time measurements, timely intervention if they appear illogical results, as well as comprehensive and rapid processing and analysis of results.

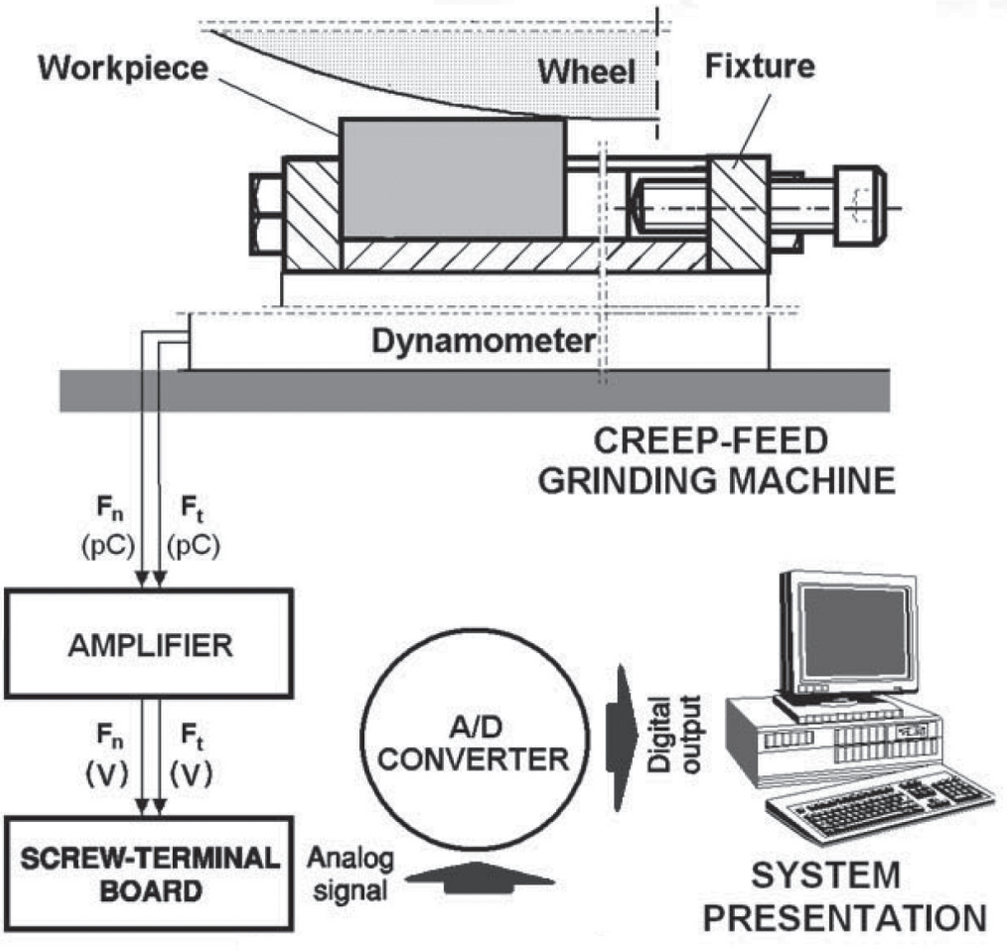

Figure 3. Information system for measuring and processing cutting forces during creep-feed grinding.

3. Analysis of experimental data

3.1. Cylindrical grinding

Based on the experimental plan and with the use of experimental devices, grinding forces values F_t and F_n are measured and recorded. Measured and calculated values for different machining parameters are shown in **Table 1**. On each sample of the material used for machining, for every experimental point, three repetitions were done, and the mean value of the repetitions was used in calculation of models.

Processing of the experimental data is performed with full factorial second-order design [9]. Side by side comparison of modeling with the genetic algorithms that were used to generate four coefficients from Eq. (1) while keeping the overall average error minimal is performed.

Table 2 contains values of regression coefficients [Eq. (1)]. It also shows the results and grades from model adequacy F_a and significance of mathematical model coefficients. Values of the coefficients which can be neglected with probability of $\alpha = 0.05$ are marked with *.

In **Table 3**, are results of modeled cutting forces with genetic algorithms are shown. **Table 4** contains exponents which are generated by genetic algorithms according the Eq. (1). Process of generating the coefficients was carried out during 5000 generations with 50 individuals. From which 5 were elite individuals and rest were created by 0.6 crossover fractions and the rest of the generation was created by mutation.

Table 5 features the comparison of success rate of these two methods of coefficients determination. Average errors in deviation of calculated resp. modeled values from experimentally obtained values are shown. It can be seen that genetic algorithms generated more suitable coefficients and thus produced smaller error for most of the forces and materials except for tangential force F_r and for steel EN 34Cr4.

From **Table 5**, it can be concluded that both techniques can be used for cutting forces modeling but genetic algorithms having a slight advantage.

Influence of cutting conditions on grinding forces $F_{t,}$ and $F_{n,}$ for both workpiece material (EN 18CrNi8 and EN 34Cr4) is shown in **Figure 4** for workpiece speed, in **Figure 5** for the feed rate and for the depth of cut in **Figure 6**.

	EN 18CrNi8		**EN 34Cr4**	
	F_t	**F_n**	**F_t**	**F_n**
C	125.3	229.8	52.03	296.1
x	0.016*	0.232	0.104	0.270
y	0.073*	0.236	0.038*	0.273
z	0.590	0.850	0.654	0.945
F_a	3.069	0.740	1.775	5.389

Table 2. Coefficients in Eq. (1), calculated by response surface methodology.

No.	Machining factor			Experimentally measured values				Modeled values by genetic algorithms			
				EN 18CrNi8		EN 34Cr4		EN 18CrNi8		EN 34Cr4	
	v_r [m/min]	s_a [mm/rev]	a [mm]	F_t [N]	F_n [N]	F_t [N]	F_n [N]	F_t [N]	F_n [N]	F_t [N]	F_n [N]
1	18.4	20	0.01	11.8	17	10.9	17.8	10.64	17.35	10.19	17.60
2	36.8	20	0.01	12.4	17.8	11.8	19.8	11.28	18.81	11.65	19.79
3	18.4	30	0.01	12.3	18.4	13	18.9	12.31	22.08	11.54	21.37
4	36.8	30	0.01	12.9	19.8	13.2	21.1	13.06	23.94	13.19	24.03
5	18.4	20	0.02	16.1	29	17.4	29	14.41	24.51	14.49	24.60
6	36.8	20	0.02	16.6	31.5	17.9	31.2	15.28	26.57	16.57	27.67
7	18.4	30	0.02	17.2	31.2	18.8	33.1	16.68	31.20	16.40	29.87
8	36.8	30	0.02	17.5	33.3	20	33.6	17.69	33.82	18.75	33.60
9	26	25	0.014	12.1	25.4	12.3	24.8	13.76	24.39	13.84	24.43
10	26	25	0.014	12	25.3	13.5	24.7	13.76	24.39	13.84	24.43
11	26	25	0.014	12.6	24.5	12.2	24	13.76	24.39	13.84	24.43
12	26	25	0.014	12.8	24.3	14	24.1	13.76	24.39	13.84	24.43
13	16	25	0.014	13.6	23.1	12.6	22.8	13.2	23.05	12.60	22.50
14	42.4	25	0.014	14.2	25.6	13.6	25.6	14.34	25.82	15.21	26.54
15	26	18.4	0.014	14.4	22.1	12.4	23.1	12.31	20.32	12.60	21.09
16	26	32.6	0.014	15.5	28.2	14.1	24.3	15.14	28.57	15.01	27.74
17	26	25	0.0086	11	19.2	10.8	19	11.11	19.13	10.80	19.31
18	26	25	0.023	17.1	33.2	18.1	31.1	17.1	31.24	17.81	31.06
19	16	25	0.014	13.4	23	12.1	22.5	13.2	23.05	12.60	22.50
20	42.4	25	0.014	14.5	25.8	13.9	25.7	14.34	25.82	15.21	26.54
21	26	18.4	0.014	14.2	22.9	12.6	23.3	12.31	20.32	12.60	21.09
22	26	32.6	0.014	15	28.1	14.6	24.1	15.14	28.57	15.01	27.74
23	26	25	0.0086	11.1	19.2	11	19.6	11.11	19.13	10.80	19.31
24	26	25	0.023	17.6	33.3	18.5	31.8	17.1	31.24	17.81	31.06

Table 3. Measured and modeled values of cutting forces.

	EN 18CrNi8		EN 34Cr4	
	F_t	F_n	F_t	F_n
C	21.165	20.637	24.130	23.674
x	0.085	0.116	0.193	0.169
y	0.361	0.595	0.306	0.479
z	0.438	0.498	0.508	0.483

Table 4. Coefficients in Eq. (1), generated with genetic algorithms.

	Response surface methodology				Genetic algorithms			
	EN 18CrNi8		EN 34Cr4		EN 18CrNi8		EN 34Cr4	
	F_t	F_r	F_t	F_r	F_t	F_r	F_t	F_r
Average error %	5.96	6.63	7.98	5.14	5.39	5.25	5.63	5.48

Table 5. Comparison of the average errors made by response surface methodology and genetic algorithms.

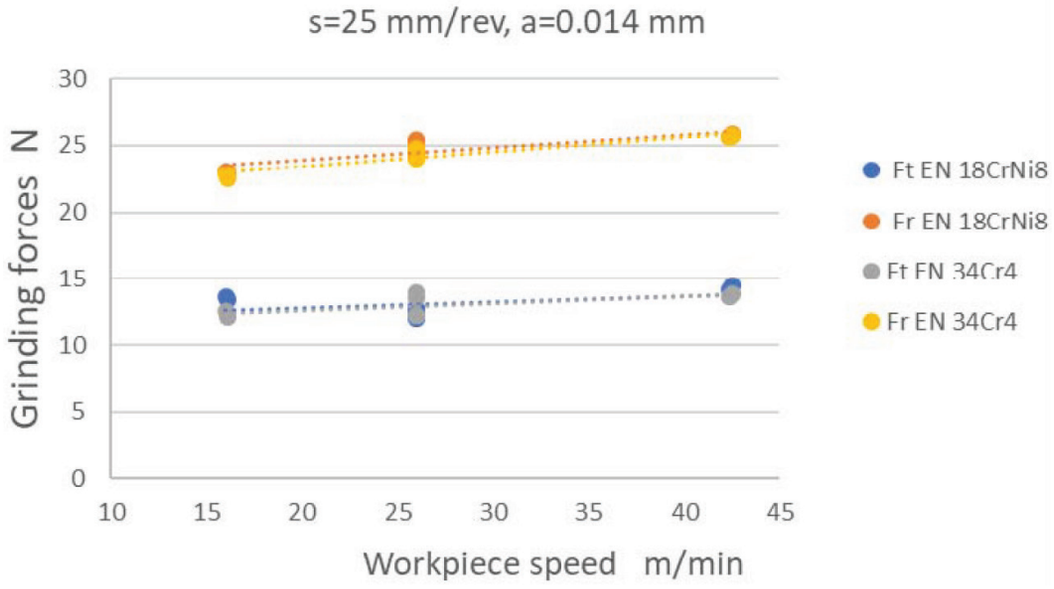

Figure 4. Influence of the workpiece speed on grinding forces.

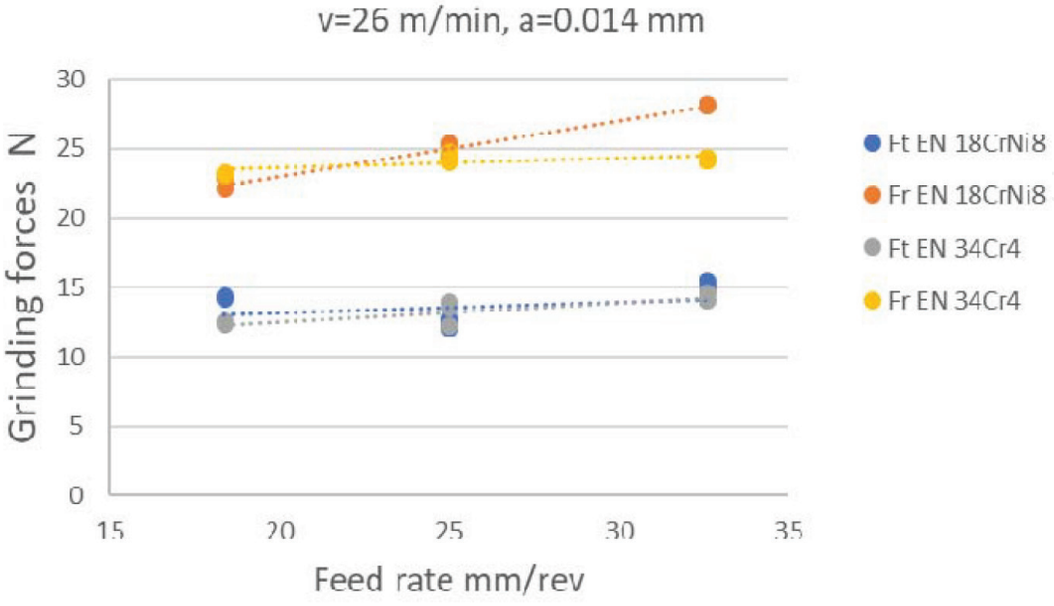

Figure 5. Influence of the feed rate on grinding forces.

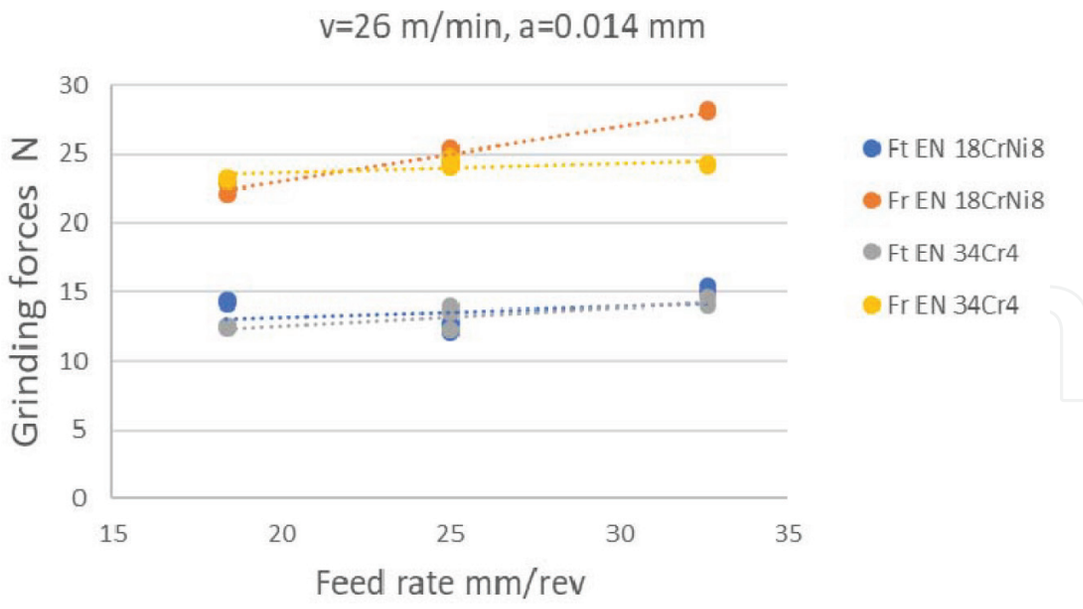

Figure 6. Influence of the depth of cut on grinding forces.

From **Figures 4–6**, it can be noticed that all input parameters, significantly influence increasing of cutting forces during cylindrical grinding process. Depth of cut has the highest influence on grinding forces followed by workpiece speed and then feed rate. This conclusion is valid for both study materials in study.

3.2. Creep-feed grinding

An example of measurement results of the cutting force during creep-feed grinding, two wheels with similar characteristics but different manufacturers, is shown in **Figure 7**. It can be concluded that for the same processing conditions obtained different values of force components sanding, or about the same dynamic character.

Figures 8 and **9** are given depending on the specific components of cutting forces, as well as their relationship F'_n/F'_t, depending on the cutting depth and the workpiece speed for both selected wheels. With diagrams shown it can be concluded that with increased cutting depth grinding forces are increasing and decrease with increasing the workpiece speed, because of cutting depth is decreasing.

Relationship of cutting force in grinding depends on the elements of the cutting regime, and a constant specific productivity of grinding, is shown in **Figure 10**. The diagram shows that compared to conventional grinding, in creep-feed grinding cutting forces appear higher for both grinding wheels.

The ratio of normal and tangential grinding forces moved to within 2–4, except that higher values related to creep-feed grinding for both grinding wheels versus the workpiece speed.

Input parameters significantly influence increase in specific cutting forces during creep-feed grinding process. Depth of cut has the highest influence on grinding forces have depth of cut,

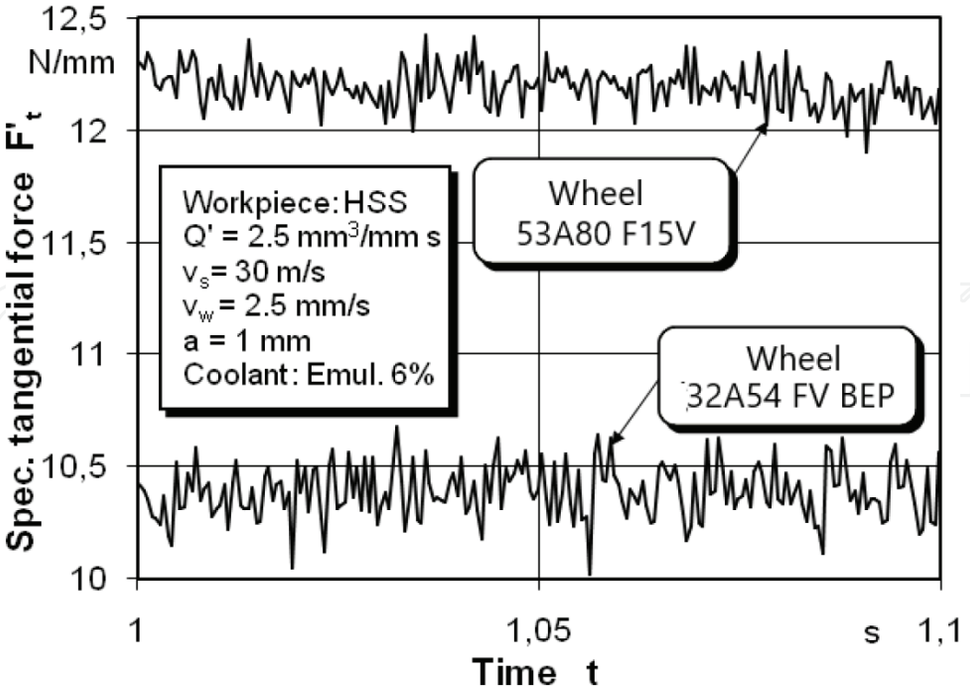

Figure 7. Value and character of the measured tangential grinding force components.

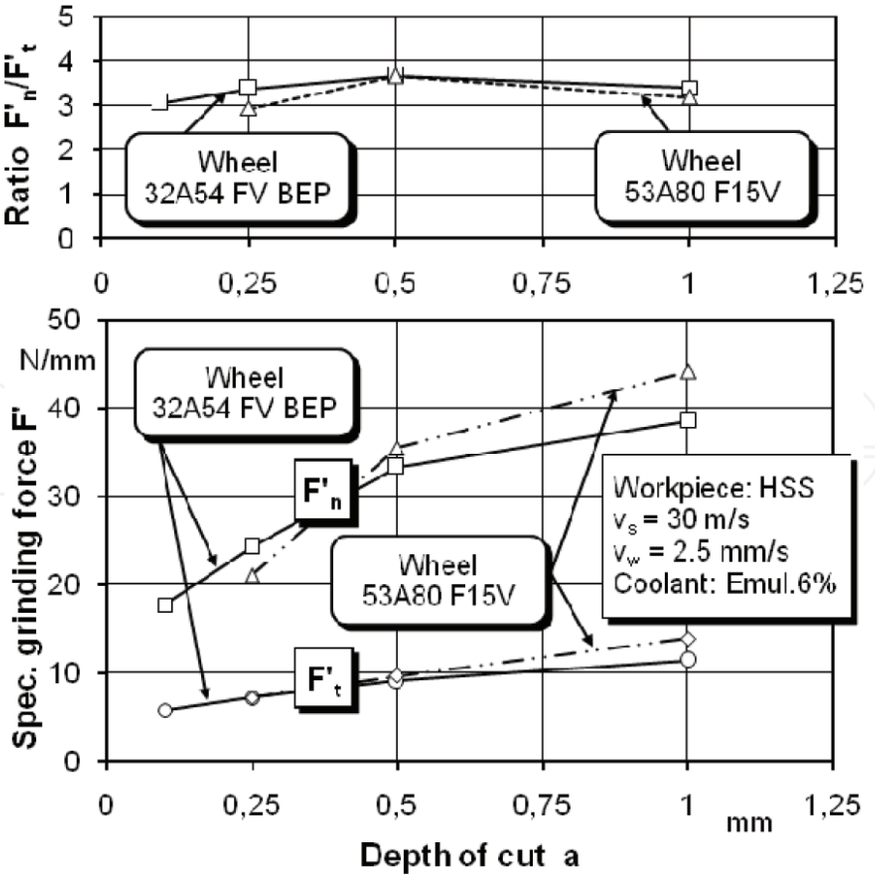

Figure 8. The grinding forces versus the depth of cut.

http://dx.doi.org/10.5772/intechopen.76968

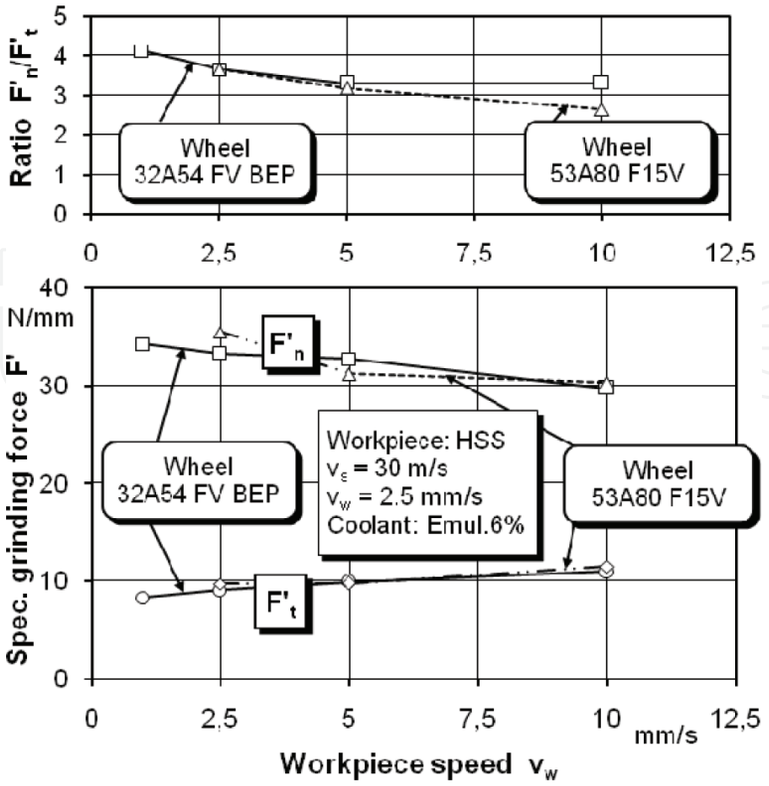

Figure 9. The grinding forces versus the workpiece speed.

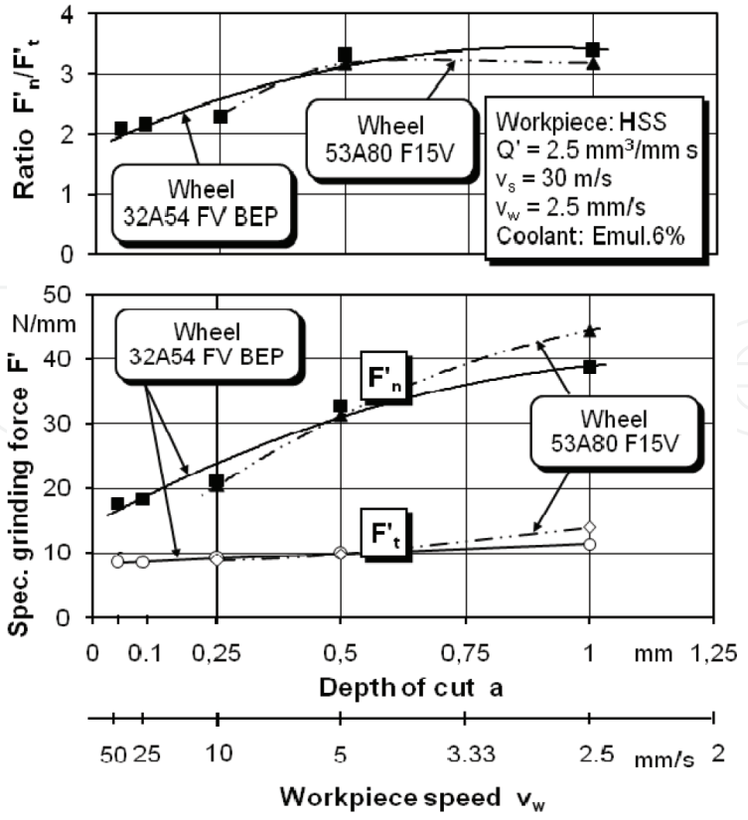

Figure 10. Specific grinding force versus the cutting regime for creep-feed grinding.

while workpiece speed has low influence on grinding forces. Increasing workpiece speed decreases specific grinding forces for both used grinding wheels.

4. Conclusions

Based on stated earlier, following can be concluded:

- Presented dynamometers can be successfully used for measurement of cutting forces during cylindrical grinding.
- Defined mathematical model of cutting forces F_t and F_r are adequate
- Influential elements of machining parameters on cutting forces are determined.
- Genetic algorithms are suitable for generating the coefficients for cutting force modeling.
- Creep-feed grinding reduces processing time, but also increases the cutting force
- Cutting forces primarily depend on the type of workpiece material and elements of its process
- Cutting forces during creep-feed grinding, due to a greater number of active abrasive grains into engagement with the workpiece material, are significantly higher compared to conventional grinding
- The grinding forces, the increasing length of contact of the grinding wheel and workpiece material, with increasing depth of cut;
- Increase the speed of the workpiece grinding forces decrease because it reduces the cross-section of the affected layers of material by grinding grain;
- Greater grinding force ratio can be observed in creep-feed;
- Cutting forces during creep-feed grinding allow identification of the energy balance of machine tools and estimation of the level of accuracy for different machining conditions

Acknowledgements

The Technological Development program Republic of Serbia, supported this TR 35015 project. For their support authors show great appreciation.

Nomenclature

v_r (m/min)	workpiece speed
s_a (mm/rev)	feed rate

a (mm)	depth of cut a (mm)
v_w (m/min)	workpiece speed creep-feed grinding
v_s (m/s)	grinding wheel speed
F_t (N)	tangential force
F_n (N)	normal force
F_a (N)	axial force
λ	grinding ratio
b	(mm) width of grinding
F_t', F_n' (N/mm)	specific grinding force:
u (n/mm^2)	specific grinding energy
h_m (mm)	grinding depth
Q′ (mm^3/mm·s)	specific material removal rate is
P′ (W/mm)	specific grinding power

Author details

Pavel Kovač* and Marin Gostimirović

*Address all correspondence to: pkovac@uns.ac.rs

Faculty of Technical Sciences, University of Novi Sad, Novi Sad, Serbia

References

[1] Rowe WB. Principles of Modern Grinding Technology. Boston: William Andrew Publishing; 2009

[2] Chang HC, Wang JJ. A new model for grinding force prediction and analysis. International Journal of Machine Tools & Manufacture. 2008;**48**:1335-1344

[3] Guo C, Campomanes M, Mcintosh D, Becze C, Green T, Malkin S. Optimization of continuous dress creep-feed form grinding process. CIRP Annals – Manufacturing Technology. 2003;**52**(1):259-262

[4] Holešovski F, Hrala M, Stančik L. Measurement of cutting forces in the centre grinder. Manufacturing Technology Journal. 2005;**5**

[5] Aslan D, Budak E. Semi-analytical force model for grinding operations. Procedia CIRP. 2014;**14**:7-12. DOI: 10.1016/j.procir.2014.03.073

[6] Patnaik Durgumahanti US, Singh V, Venkateswara Ra P. A new model for grinding force prediction and analysis. International Journal of Machine Tools and Manufacture. 2010;**50**(3):231-240

[7] Yao C, Wang T, Xiao W, Huang X, Ren J. Experimental study on grinding force and grinding temperature of Aermet 100 steel in surface grinding. Journal of Materials Processing Technology. 2014;**214**:2191-2199

[8] Kopač J, Krajnik P. High-performance grindig – A review. Journal of Materials Processing Technology. 2006;**175**(1-3):278-284

[9] Liu Q, Chenb X, Wangc Y, Gindy N. Empirical modelling of grinding force based on multivariate analysis. Journal of Materials Processing Technology. 2008;**203**:420-430

[10] Gostimirovic M, Sekulic M, Kopac J, Kovac P. Optimal control of workpiece thermal state in creep-feed grinding using inverse heat conduction analysis. Strojniški vestnik – Journal of Mechanical Engineering. 2011;**57**(10):730-738

[11] Gostimirovic M, Kovac P, Jesic D, Skoric B, Savkovic B. Surface layer properties of the workpiece material in high performance grinding. Meta. 2012;**51**(1):105-108

[12] Gostimirovic M, Kovac P, Sekulic M. An inverse heat transfer problem for optimization of the thermal process in machining. Sadhana. 2011;**36**(4):489-504

[13] Kovač P. Modeling of Machining Process- Factorial Experimental Plans (in Serbian). Novi Sad: FTS; 2006

[14] Pucovski V, Kovač P, Tolnay M, Savković B, Rodić D. The adequate type of function for modeling tool life selection by the use of genetic algorithms. Journal of Production Engineering. 2012;**15**(1):25-28

[15] Mishra VK, Salonitis K. Empirical estimation of grinding specific forces and energy based on a modified Werner grinding model. Procedia CIRP. 2013;**8**:287-292